Journal of the Indian Chemical Society 99 (2022) 100271

Contents lists available at ScienceDirect

Journal of the Indian Chemical Society

journal homepage: www.editorialmanager.com/JINCS/default.aspx

A sustainable method of mitigating acid corrosion of mild steel using jackfruit pectin (JP) as green inhibitor: Theoretical and electrochemical studies

Shamsheera K O, Anupama R Prasad, Muhammed Arshad, Abraham Joseph *

Department of Chemistry, University of Calicut, Calicut University P O, Kerala, India

ARTICLE INFO

Keywords:
Jackfruit pectin
Monte Carlo simulation
Surface studies
Impedance

ABSTRACT

This study is attempted to develop a green corrosion inhibitor from a waste material of Jack fruit (*Artocarpus heterophyllus*). This method is therefore quite valuable to health, environment, and economic point of view. Pectin is isolated from the jackfruit peel waste using 0.05 N oxalic acid and used as an inhibitor for mild steel corrosion in acidic environment as it is highly water soluble. 250–1000 ppm of pectin was used in this study at a temperature range of 303–323 K. The protection efficiency of jack fruit pectin (JP) in 0.5 M HCl was evaluated by conventional weight loss and electrochemical techniques. The potentiodynamic polarization results revealed that JP could effectively reduce the corrosion of mild steel in acidic medium at 1000 ppm concentration with an inhibition efficiency of 89.75% and corrosion rate of 2.392 mpy. The mixed type behavior of the inhibitor is identified from Tafel polarization studies. Electrochemical impedance spectroscopy (EIS) measurements suggest that the corrosion inhibition process is kinetically controlled. adsorption and kinetic behavior of the inhibitor also have been studied. Surface manifestations were followed using FESEM and AFM techniques. DFT calculations and Monte Carlo simulations were also carried out to corroborate the experimental results with theoretical outputs and succeeded to a great extent.

1. Introduction

The spontaneous deterioration of a metal/material is playing a pivotal role in the economy and safety of nations directly or indirectly. Mankind cannot even imagine a world without metals and alloys. Mild steel is one of the most widely used engineering and construction material owing to its incomparable mechanical properties and cost-effectiveness over others [1]. However, as the passive oxide layer of MS is highly porous and incompetent like most of the other metal oxides, the chance of getting corroded under the corrosive environment is very high. Acid media, particularly HCl are widely used in various industrial processes such as oil well acidification, acid pickling of steel and iron, chemical cleaning, and processing. HCl is more cost effective and benign when compared to other mineral acids [2]. The addition of suitable benign inhibitors containing lone pair of electrons and multiple bonds can prevent the corrosion process to a great extent by the interaction between the metal atom and the inhibitor molecules [3,4]. Most of the organic and inorganic inhibitors are not environmentally benign though the hazardous index varies from case to case. In the context of developing and maintaining a green environment, the focus is not only on the inhibition efficiency but also on its origin. The use of plant extract as corrosion inhibitor got much attention during these years is mainly due to these reasons. The enhanced protective action of plant extracts is due to the presence of verities of phytochemicals [5,6]. M. Dahmani et al. reported the corrosion inhibition of C38 steel in 1 M HCl by isolating piperine from black pepper extract [7]. The compound apigetrin isolated from *matricaria aurea* extracts was used as an effective green inhibitor for MS in 1 M HCl [8]. Carbohydrate polymers extracted from natural sources have also been used as good corrosion inhibitors for various metals in different aggressive media [9]. Pectin, a heteropolysaccharide with carboxylic and carboxymethyl functional groups is considered a promising candidate for the corrosion inhibition of common metals, especially at ambient temperature conditions. For instance, Grazino et al. used tomato peel waste as a potential source of pectin from canning industries for the corrosion inhibition of tin in a mixture of 2% NaCl, 1% acetic acid, and 0.5% citric acid media [10] and Jasna et al. isolated pectin from tomato peel waste and corrosion inhibition of tin was carried out in sodium chloride/acetic acid medium [11]. Subarkah et al. have reported corrosion inhibition for

* Corresponding author.
E-mail address: abrahamjoseph@uoc.ac.in (A. Joseph).

https://doi.org/10.1016/j.jics.2021.100271
Received 6 July 2021; Received in revised form 4 November 2021; Accepted 17 November 2021
0019-4522/© 2021 Indian Chemical Society. Published by Elsevier B.V. All rights reserved.

mild steel using pectin extracted from fresh lemon peel [12]. Xuemei et al. isolated pectin from sunflower head by enzyme assisted extraction and offer an inhibition efficiency of 92.05% at its optimum concentration of 2 g/L [13]. Jack fruit (*Artocarpus heterophyllus*), known as the poor man's fruit is one of the largest edible fruits grown worldwide. But a significant amount of jack fruit peel is discarded as waste, leading to environmental problems [14]. Suitable procedures can be used to convert these discarded wastes into value-added products. By-product recovery from fruit wastes not only can improve the overall economics of processing units but also reduce the problem of environmental pollution considerably. Recovery/isolation of valuable ingredients/compounds from agricultural waste and by-product is a novel research movement that got greater attention. Pectin is a valuable by-product that can be isolated from jack fruit waste using different techniques [15]. Begum et al. isolated the highest yield of pectin from jack fruit waste using sodium hexametaphosphate [16]. In another study, Koh et al. used different power levels of microwave-assisted procedures for extracting pectin from jackfruit waste with 17.63% yield [17]. Pectin from jack fruit waste was also extracted by Xu et al. via ultrasonic-microwave-assisted extraction with citric acid and the yield was 21.5% [14]. Sundarraj et al. used different acids for isolating pectin from jack fruit waste and got the highest yield of 38% with 0.05 N oxalic acid [18]. According to Yujaroen et al. and Chandel et al., oxalic acid was the best solvent for extracting pectin from jackfruit peel waste [19]. So, in this study, we used oxalic acid for extracting JP from jack fruit peel waste according to the procedure of Sundarraj et al. The purpose of this study was to utilize jack fruit peel waste as a potential source for JP and use it as a corrosion inhibitor for MS in the acid environment so that it will be quite beneficial to the environment and economy. To the best of our knowledge, this is the first comprehensive study including experimental and theoretical studies on the use of JP as a corrosion inhibitor for MS in HCl media.

2. Materials and method

2.1. Materials

Jack fruit peel waste with conical carpel apices was manually peeled off and washed thoroughly with water to remove the adhesive waste if any present on the surface. Then the peels were finely chopped, washed, and blanched at 80 °C for 15 min, and dried in a hot air oven at 60 °C until it registers the stable weight. The dried peels were pulverized using a grinder and passed through a 40-mesh sieve and powdered samples were kept in polyethylene bags and stored at room temperature. Analytical grade solvents and chemicals were used in this work and were obtained from Merck chemicals. The medium for the study was prepared from reagent grade samples on proper dilution supplied by E Merck.

The MS samples used in this study comprised of about 98.75% of Fe, ≈1% of Mn; 0.2% of C; 0.03% of P; ≈ 0.02% of S. The MS coupons were polished with various grades of emery papers and cleaned with ethanol, acetone, and finally with distilled water as proposed by ASTM standard G-1-72 procedure before each measurement [20].

2.2. Extraction of JP from jackfruit peel powder

Sundarraj et al. have already established that oxalic acid is the best acid for the extraction of pectin from jack fruit peel waste with a high yield [18]. Briefly, 25 g of the ground jackfruit peel powder was added into a beaker containing 250 mL of 0.05 N oxalic acid. Then the mixture was stirred in a water bath for 60 min at 90 °C. The oxalic acid extract was filtered through a muslin cloth. The filtrate was cooled to room temperature. Then 95% ethanol was added to the cold solution and allowed the pectin to precipitate. The precipitate was collected and dried at 50 °C for 24 h. The pectin yield was calculated using the following equation [21].

$$yield(\%) = 100 \times P/_{Bi} \quad (1)$$

where P is the weight of extracted JP in gram and Bi is the initial amount of jackfruit peel powder (25 g). The light brown coloured pectin was used for corrosion inhibition studies.

2.3. Characterization of J-Pectin

Spectroscopic techniques were used to characterize the structure of pectin extracted from jack fruit peel. The MS coupon was dipped in 0.5 M HCl containing 1000 ppm of JP for 24 h. Then the coupons were released from the medium, washed with water, and dried at room temperature. The adsorbed JP on the metal coupons were scraped out and pelletized with KBr and FTIR spectrum was recorded.

2.4. Corrosion study

For weight loss studies the freshly prepared flat MS coupons with an area of 2 × 1.8 cm^2 were accurately weighed and immersed in 0.5 M HCl containing different concentrations of JP ranging from 250 to 1000 ppm. After 24 h of immersion, the MS coupons were taken out from the corrosive medium and the metal coupons were washed thoroughly with water, dried, and then weighed. From the weight loss, the corrosion rate (CR) was calculated using the following equation [22].

$$CR = \frac{W}{A \times t} \quad (2)$$

where W is the weight loss of MS in mg after dipping in corrosive medium, A is the area of dipped MS coupon and t is the dipping time in hours. The percentage inhibition efficiency (IE) was calculated from weight loss of MS coupons in the absence and presence of JP (W_o and W_i) by

$$IE(\%) = \frac{W_0 - W_i}{W_0} \times 100 \quad (3)$$

The surface coverage (θ) was calculated to realize the adsorption of JP on MS surface by replacing the pre-adsorbed water molecule using the following equation

$$\theta = \frac{IE}{100} \quad (4)$$

2.5. Electroanalytical studies

Electrochemical impedance spectroscopy (EIS) and potentiodynamic polarization (PDP) measurements were carried out using a three-electrode cell set up and Gill AC electrochemical work station. The working electrode was MS specimen with 1 cm^2 exposed area, a saturated calomel electrode as the reference electrode with a Luggin capillary to minimize the IR drop at the working electrode, and a platinum counter electrode. The MS working electrode was vertically immersed in 0.5 M HCl solution in the absence and presence of JP for 1 h and OCP (open circuit potential) was evaluated from the time vs potential curve. When potential became nearly constant (<5 mV) to time, electrochemical measurements were carried out. Impedance analysis was performed with a minimum amplitude of 10 mV at a frequency domain from 0.1 Hz to 10 kHz. The data obtained from the EIS plot were assessed by using Z simp win. The potential of PDP curves was recorded from potential −250 mV to +250 mV with regard to the OCP at 60 mV/min scan rate.

2.6. Surface characterization

The MS specimen immersed in 0.5 M HCl in the absence and presence of 1000 ppm of JP for 24 h was used for surface studies. The coupons were taken out from the electrolyte and washed thoroughly with distilled

water, dried at room temperature, and subjected to FESEM with CARL ZEISS MODEL FESEM. To evaluate the roughness on the metal surface in the absence and presence of 1000 ppm of JP, AFM topography was taken and analysed using NTEGRA PRIMA Atomic Force Microscope in non-contact mode.

2.7. Quantum chemical study

The preliminary theoretical calculations on pectin were done using Gaussian 09 package. DFT/B3LYP/6-311G (d, p) method was used to optimize the geometry of pectin and single-point energy calculations. Frontier molecular orbitals (HOMO and LUMO) were used to interpret the adsorption of JP on the MS surface. The E_{HOMO} and E_{LUMO} values were used to determine IP (ionization potential) and EA (Electron affinity) using the equations [23].

$$Ionization\ \ potential(IP) = -E_{HOMO} \tag{5}$$

$$Electron\ \ affinity(EA) = -E_{LUMO} \tag{6}$$

From IP and EA, the global descriptive parameters η (hardness), and χ (electronegativity) are determined by Koopman's theorem [24].

$$Absolute\ \ Hardness\ (\eta) = \frac{IP - EA}{2} \tag{7}$$

$$Absolute\ \ Electronegativity(\chi) = \frac{IP + EA}{2} \tag{8}$$

The application of Pearson's method permits the assessment of the electron transfer tendency of an inhibitor to the metal specimen from the number of electrons transferred from the following equation [25].

$$\Delta N = \frac{\Phi - \chi_{inh}}{2(\eta_{Fe} + \eta_{inh})} \tag{9}$$

where Φ and χ_{inh} are the work function and electronegativity of inhibitor, η_{Fe} and η_{inh} denote the absolute hardness of Fe metal and the JP. A theoretical value of η_{Fe} is used as zero (since for bulk metallic atoms IP = EA) and the value of Φ for Fe (110) is frequently used as 4.82 [26,27]. The natural bonding orbital (NBO) analysis was accomplished using NBO 3.1 as enabled in the Gaussian 09 at the DFT/B3LYP/6-311G (d, p) level to achieve natural charge via natural population analysis. Condensed Fukui functions via finite difference approximation from natural population analysis were used to interpret both nucleophilic and electrophilic centres on the inhibitor JP. The Fukui functions were calculated as follows [28–31].

$$f_k^+ = qk(N+1) - qk(N) \tag{10}$$

$$f_k^- = qk(N) - qk(N-1) \tag{11}$$

where qi(N+1), qi(N), and qi(N-1), are the atomic charges of the system with N+1, N, and N-1 electron.

2.8. Monte Carlo simulation studies

Monte Carlo simulation is used to compute the interaction energy of inhibitor with the metal surface and to find the best stable adsorption configuration. To understand the mode of adsorption of JP on the Fe (110) plane, Monte Carlo simulation was carried out via the BIOVIA material studio programme. All constituents of simulation systems were optimized by the Forcite module using the COMPASS forcefield. The builder module of the material studio was used to construct the crystal structure of Fe. The Fe crystals were cleaved along (1 1 0) plane. Fe (1 1 0) plane is selected owing to its highly packed structure and high stabilization energy. To provide better interaction of JP and water with Fe surface, 12 × 12 supercells were designed using the builder module. A vacuum slab with 10A^o thickness was built. The COMPASS Force field was used to relax the Fe (1 1 0) surface [32,33]. To mimic the experimental condition, a single molecule of optimized JP along with 190 molecules of water and $4H_3O^+$, 4 Cl^- were made to adsorb onto the Fe (110) surface introduced onto the Fe (110) surface via the adsorption locator module.

3. Discussion

3.1. Yield of pectin

Antony et al. could isolate about 39.05% of pectin from jack fruit waste using 0.05 N oxalic acid at 90 °C for 60 min. But in this study, we could produce only 35.05% only using the same condition. The low yield of pectin might be due to environmental growth conditions and the variety of the jack fruit used in this study. The isolated pectin is soluble in 0.5 M HCl with some insoluble portions as the concentration increases. The low solubility is due to the decrease in the degree of esterification.

3.2. FTIR

The FTIR spectra of JP and JP scraped from the metal surface after 24 h of exposure in 0.5 M HCl are given in Fig. 1. Absorption of about 3426 cm^{-1} arises due to the O–H stretching frequency of the polysaccharide unit. The carbonyl stretching frequency of the methyl ester group in pectin got registered at 1744 cm^{-1}. The carbonyl stretching frequency of the carboxyl group in galacturonic acid appeared at 1639cm-1. The asymmetric and symmetric C–H stretching frequency of methyl esters of galacturonic acid appeared at 2924 cm^{-1} and 2830 cm^{-1}. The spectra of JP adsorbed on the MS surface show a decrease in intensity of O–H stretching and bending frequency due to the association of the JP molecule with the surface of metal [10,34,35]. The intensity of carbonyl stretching frequency of acid and ester group in JP at 1744 cm^{-1} and 1639 cm^{-1} get decreased upon complex formation with the metal atom.

3.3. Weight loss measurement

The CR and IE of MS obtained from the weight loss study for various concentrations of JP are exhibited in Table 1 and the data indicated that CR of MS decreased with an increase in the concentration of JP. The inhibition of MS corrosion in the presence of JP is attributed to the adsorption of the inhibitor molecule on the surface of the metal atom by replacing pre-adsorbed water molecules, which offers a barrier to corrosive ions to reach the target sites. At higher concentration, the inhibitor

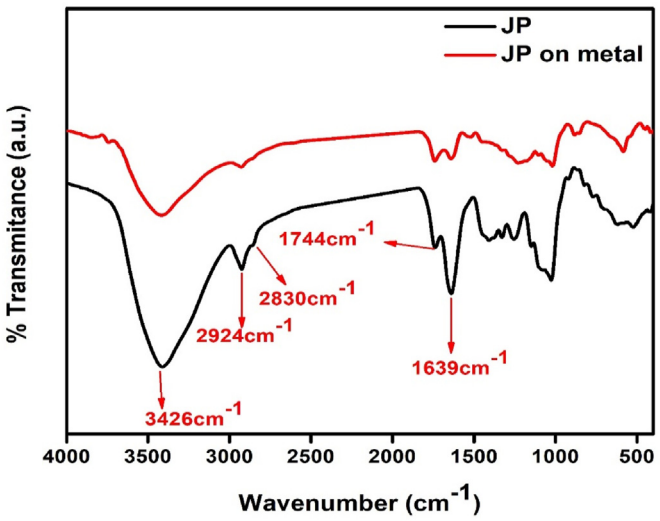

Fig. 1. FTIR spectra of JP and JP on MS after 24 h immersion in 0.5 M HCl.

Table 1
Weight loss data of MS in 0.5 M HCl in the absence and presence of JP after 24 h of immersion.

Concentration of Pectin (ppm)	Weight loss (g)	CR (mg cm^{-2} hr^{-1})	IE (%)	(θ)
Blank	0.4256	4.925		
250	0.1256	1.453	70.49	0.7049
500	0.0862	0.9976	79.74	0.7974
750	0.0443	0.5127	89.59	0.8959
1000	0.0343	0.3969	91.94	0.9194

molecule could form a protective film of JP which inhibit the diffusion of electrolyte from aggressive media onto the metal surface. Maximum surface coverage and hence maximum IE were observed at 1000 ppm of pectin.

3.4. Electrochemical measurements

3.4.1. Open circuit potential (OCP)

OCP is the potential generated over the MS relative to the reference electrode without applying any external current or potential. The variation of OCP with time for MS in 0.5 M HCl in the absence and presence of a different concentration of JP from 303 to 323 K are shown in Fig. S_1. For better interpretation and consistency of the OCP curves, the OCP studies for MS dissolution in 0.5 M HCl were done for 180 s. The OCP versus time curves is almost straight throughout the experiments for MS in the absence and presence of JP. The shift in OCP versus time curves of inhibited MS samples with respect to uninhibited sample gives information about the nature of the inhibitor [36]. The OCP versus time curves for MS inhibited by JP are shifted towards more positive values, indicating the development of a protective film of JP on the surface of MS [37].

3.4.2. EIS measurements

The electrochemical corrosion study of MS in 0.5 M HCl in the absence and presence of different concentrations of JP from 303 to 323 K was investigated using the EIS technique as shown in Fig. 2. To find out the most equivalent circuit that fits the experimental results, the EIS data were fitted with an appropriate equivalent circuit using Zsimp win software. A simple Randel's circuit gave the best fit to impedance data in which a constant phase element (CPE) instead of double-layer capacitance (C_{dl}) is used to fit more accurately the impedance behaviour of the electric double layer. The parameters comprised of solution resistance (R_s), and charge transfer resistance (R_{ct}) in parallel with CPE (Q_{dl}) representing C_{dl}. The values of C_{dl} could be obtained from R_{ct} and CPE parameters (Q_{dl} and n) as follows [24].

$$C_{dl} = \sqrt[n]{Q \times R_{ct}^{1-n}} \tag{12}$$

The decrease in C_{dl} values of MS in the presence of JP compared to the uninhibited solution is due to decreased dielectric constant at the metal electrolyte interface and hence better adsorption of JP on the surface of MS. The corrosion inhibition performance of JP on MS was calculated using R_{ct} values as follows [38].

$$IE(\%) = \frac{R_{ct}^{*} - R_{ct}}{R_{ct}^{*}} \tag{13}$$

where R_{ct}^{*} and R_{ct} are charge transfer resistance of electrolyte in the presence and absence of JP. Effective corrosion resistance is associated with low C_{dl} value and high R_{ct} values. The EIS data reported in Table 2 showed that R_{ct} value increases with increasing the concentration of JP with respect to the blank, and C_{dl} values tend to decrease, clearly indicated that the IE increases with an increase in JP concentration. At 1000 ppm the JP molecule forms a more efficient protective film on the MS surface and blocks the diffusion of aggressive ions from the electrolyte. Moreover, with an increase in temperature from 303 K to 323 K, the C_{dl}

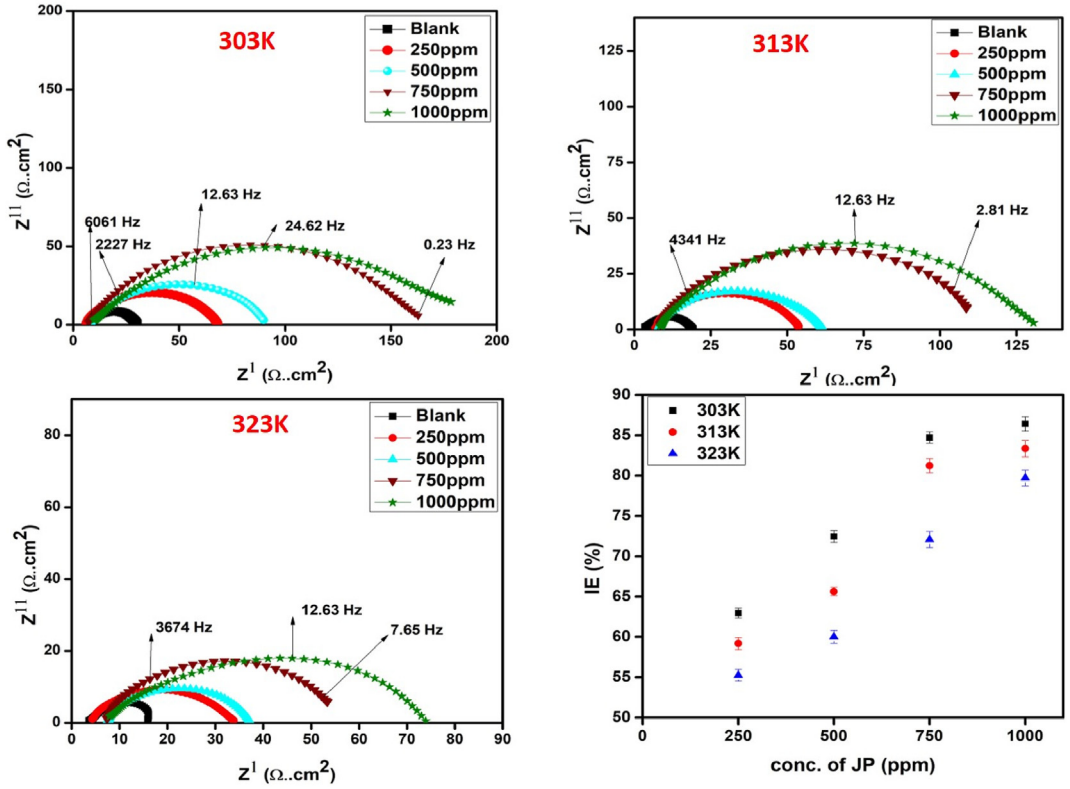

Fig. 2. EIS plot of MS in 0.5 M HCl in the absence and presence of different concentrations of JP from 303 to 323 K and the associated error bar to denote standard deviation.

Table 2
Parameters obtained from EIS plot of MS in 0.5 M HCl in the absence and presence of different concentration of JP from 303 to 323 K.

Temperature	Concentration of JP (ppm)	R_s (Ωcm^2)	R_{ct}(Ωcm^2)	n	$Q_{dl} \times 10^{-4}$ $S^n\ \Omega^{-1}\ cm^{-2}$	C_{dl}($\mu F\ cm^{-2}$)	CR (mpy)	IE (%)	Standard deviation
303K	Blank	7.01	22.84	0.80	10.59	417.6	13.24		
	250	6.24	62.51	0.80	6.257	278.2	4.837	63.46	0.6070
	500	7.69	84.63	0.79	5.399	275.0	3.573	73.01	0.7261
	750	7.65	159.7	0.77	3.961	271.9	1.893	85.69	0.6894
	1000	7.8	183.3	0.77	3.631	253.1	1.649	87.53	0.8981
313K	Blank	5.02	18.91	0.80	15.4	636.1	15.99		
	250	6.80	47.29	0.76	6.125	366.9	6.393	60.01	0.7428
	500	7.74	56.20	0.77	5.665	313.4	5.578	66.35	0.5269
	750	7.42	105.3	0.76	4.293	295.9	2.871	82.04	0.8907
	1000	7.73	123.7	0.76	3.794	264.6	2.440	84.71	1.016
323K	Blank	3.571	13.19	0.78	16.57	757.1	22.92		
	250	7.84	29.98	0.76	9.530	568.3	10.08	56.00	0.7134
	500	7.19	33.81	0.74	5.590	345.0	10.01	60.98	0.8047
	750	6.78	49.43	0.77	6.125	337.4	6.117	73.31	1.021
	1000	7.34	67.94	0.75	4.511	304.1	4.450	80.58	0.9805

values increases, and R_{ct} values decrease, and hence IE decreases, which is attributed to the desorption of JP molecule from the MS surface at higher temperatures. 1000 ppm of pectin extracted from jack fruit peel waste could provide 87.53% at 303 K in 0.5 M HCl. The reproducibility of both corrosion rate and inhibition efficiency is confirmed by conducting the experiments in triplicate.

3.4.2.1. Isotherm evaluation. The corrosion inhibition of metal mainly depends on the tendency of an inhibitor molecule to adsorb on the metal surface by substituting pre-adsorbed water molecules. JP donates its free electrons to the vacant d orbital of the metal atom and forms a protective layer due to effective adsorption [39]. Data obtained from the EIS study were used for fitting Frumkin, Temkin, and Langmuir isotherm models. In this case, the linear regression coefficient (R^2) at studied temperatures indicates that the adsorption of JP onto the surface of MS is in agreement with Langmuir adsorption which gave the best fit (Fig. 3). The degree of surface coverage (θ) increases with increasing the concentration of JP and decreases with a rise in temperature from 303 K to 323 K. The Langmuir isotherm model is formulated as [24].

$$\frac{C_{inh}}{\theta} = \frac{1}{K_{ads}} + C_{inh} \tag{14}$$

where C_{inh} is the concentration of JP used in the corrosive medium, and

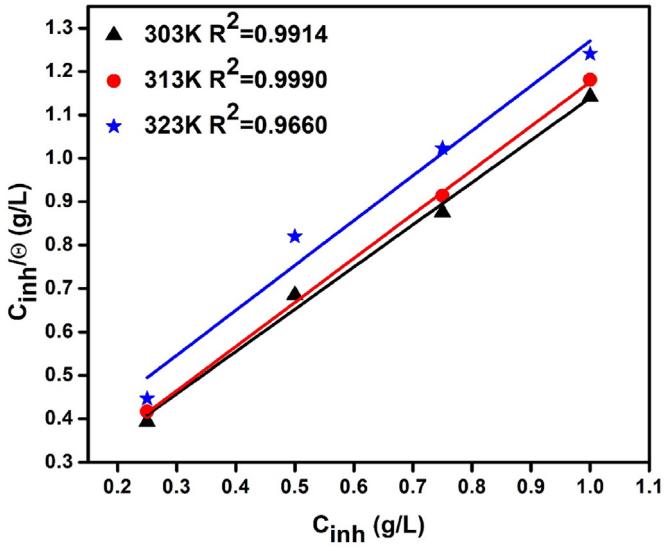

Fig. 3. Langmuir adsorption isotherm for MS at different temperature in 0.5 M HCl.

K_{ads} is the adsorption-desorption equilibrium constant. From the intercept of the C_{inh}/θ versus C_{inh} plot, K_{ads} was calculated for the adsorption of JP on the MS surface. The value of K_{ads} may be taken as the strength of the adsorption forces between the metal surface and the inhibitor molecule. The relatively high K_{ads} value (6.05 L/mg) at 303 K shows effective adsorption of JP on the MS surface, which allows better shielding and hence better anti-corrosion nature which gets reduced to 4.24 L/mg on raising the temperature to 323 K. The free energy of adsorption (ΔG^0_{ads}) is related to the K_{ads} with the equation [40].

$$\Delta G^0_{ads} = -RTln(K_{ads} \times C_{solvent}) \tag{15}$$

where $C_{solvent}$ is the solvent concentration. Table S_1 contains the value of ΔG^0 and K_{ads} at different temperatures. The spontaneous adsorption of JP on the surface of MS is clear from the negative value of ΔG^0. It is established that the value of ΔG^0_{ads} is around −40 kJ/mol or more negative are regarded as chemisorption, and if it is around −20 kJ/mol or lower are regarded as physisorption. Chemisorption is due to the development of the coordinate type bond between the lone pair of electrons in the inhibitor and the vacant d orbital of the metal atom. The electrostatic interaction of the charged metal and the inhibitor molecule results in physisorption. So, it can be realized from the ΔG^0 values that the JP adsorbed physically on the MS surface. The physisorption may arise through the electrostatic interaction of polarized iron surface with partially polarized oxygen atoms of JP, accompanied with the displacement of pre-adsorbed water molecules, leading to the development of protective layers against corrodent.

3.4.2.2. Thermodynamic and activation parameters. To evaluate the mechanism of the adsorption process, thermodynamic parameters of adsorption were calculated using the CR from the EIS measurements at an elevated temperature ranging from 303 to 323 K. The temperature rise may cause the decomposition of the protective layer, surface etching, and the desorption of the inhibitor molecules from the MS surface, and thereby increasing the corrosion rate [23]. The value of apparent activation energy (Ea) of the corrosion process was calculated using the Arrhenius rate equation

$$log(CR) = \frac{-E_a}{2.303RT} + logA \tag{16}$$

where A is the Arrhenius constant, T absolute temperature, and R is the molar gas constant. The plot of log (CR) vs 1/T gave a straight line (Fig. 4A) with slope $-E_a/2.303R$ and the calculated Ea values are given in Table S_2. The Ea value of the corrosion process of MS in the presence of JP is higher than the uninhibited acid solution. The higher E_a obtained for 1000 ppm of JP discloses that better surface coverage is offered by JP molecules via strong adsorption and thereby increases the energy barrier

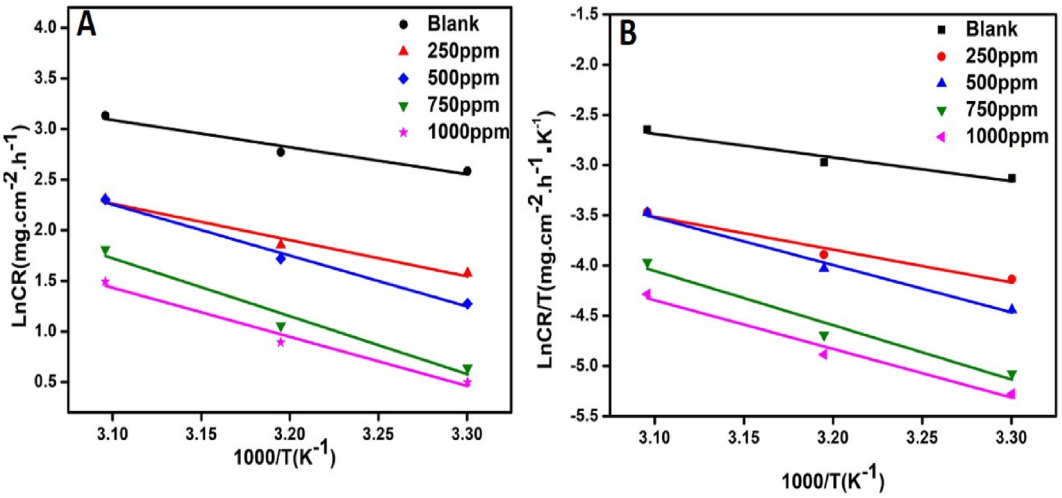

Fig. 4. (A) Arrhenius and (B) Transition state plots of MS in 0.5 M HCl with various concentrations of JP.

for the metal dissolution process.

To further elucidate the inhibitive mechanism, thermodynamic parameters like the entropy of adsorption (ΔS), and the enthalpy of adsorption (ΔH) for the corrosion process were derived according to the Transition state equation:

$$CR = \frac{RT}{Nh}\exp\left(\frac{\Delta S}{R}\right)exp\left(\frac{-\Delta H}{RT}\right) \quad (17)$$

where N is the Avogadro's number and h Planck's constant. The plots of log (CR/T) versus 1/T for the blank and varying concentration of JP gave a straight line (Fig. 4B) with a slope of (-ΔH/2.303R) and an intercept of (log(R/Nh) +ΔS/2.303R) from which entropy and enthalpy of adsorption for the corrosion process were calculated and are given in Table S_2. Higher positive values for ΔH in presence of 1000 ppm of JP imply the endothermic nature of the metal dissolution process and difficulty in triggering the reaction to cause corrosion [41]. Similarly, the high positive values of ΔS for 1000 ppm of JP indicate that in the rate-determining step, the activated complex signifies dissociation and disordering from the reactants to the activated complex [42].

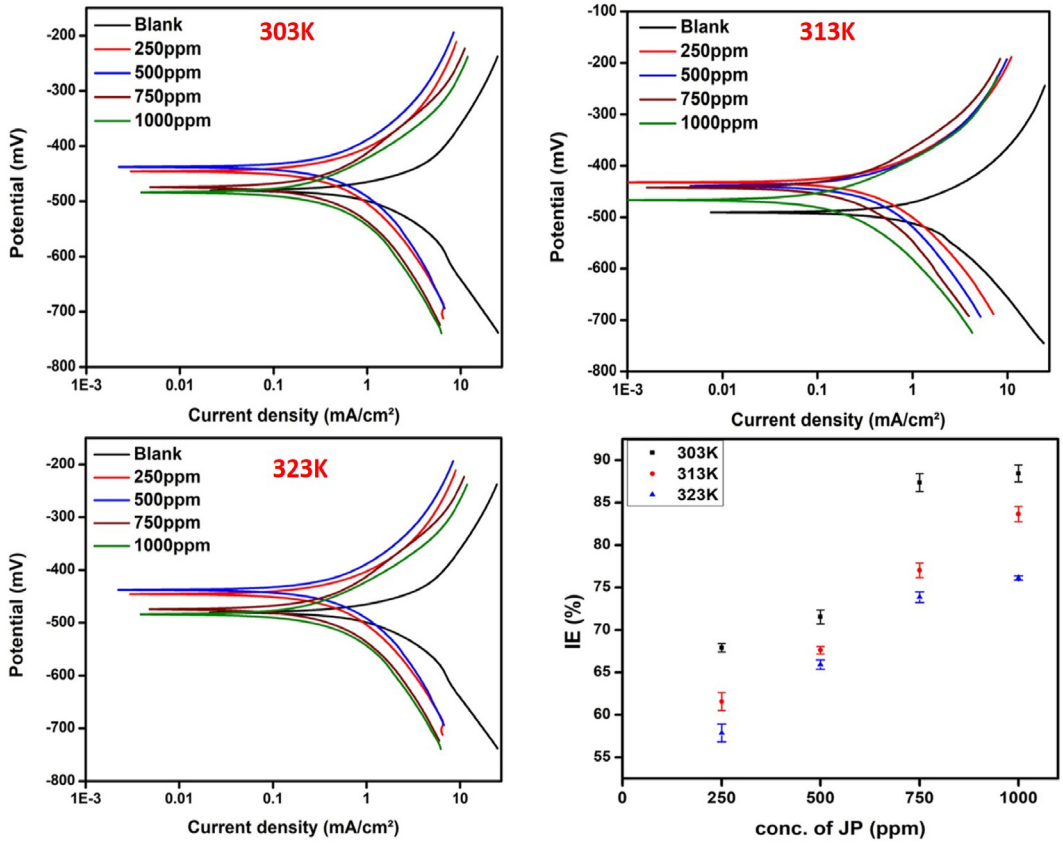

Fig. 5. PDP plot of MS in 0.5 M HCl in the absence and presence of different concentrations of JP from 303 to 323 K and the associated error bar to denote standard deviation.

3.4.3. Potentiodynamic polarization study

The corrosion performance of MS in the absence and presence of a varying concentration of JP from 303 K–323 K was studied using the PDP technique and is given in Fig. 5. Corrosion potential (E_{corr}), and corrosion current density (I_{corr}) obtained by extrapolating the Tafel lines to the E_{corr}, and anodic and cathodic Tafel slopes (βa and βc) deduced from the PDP data are given in Table 3. These results reveal that the value of I_{corr} and CR decline with an increase in JP concentration, designating that the JP molecule could inhibit corrosion by adsorbing firmly on the MS surface and blocking the movement of corrosive ions from the electrolyte. The I_{corr} value obtained for MS in the presence of JP (0.1329 mA/cm^2 at 1000 ppm) is very lower compared to the blank solution(1.2973 mA/cm^2). With increasing the temperature from 303 K to 323 K, the I_{corr} and CR increase, which can be attributed to the desorption, dissociation, and rearrangement of the inhibitor on the metal surface. It was also observed that the addition of the JP affects both the anodic metal dissolution and cathodic hydrogen evolution, which implies that JP act as a mixed type inhibitor for mild steel corrosion in 0.5 M HCl. The magnitude of the shift in E_{corr} values (<85 mV) further corroborates the mixed type behaviour of JP. The IE was calculated using the I_{corr} values using the following equation

$$IE(\%) = \frac{I^*_{corr} - I_{corr}}{I^*_{corr}} \quad (18)$$

where I^*_{corr} and I_{corr} are corrosion current density of MS in the absence and presence of pectin. The maximum efficiency of 89.75% was observed at the JP concentration of 1000 ppm at 303 K. Polarization resistance (R_p) using the Stern-Geary equation [43] was also calculated using equation (19).

$$R_p = \frac{\beta_a \beta_c}{2.303(\beta_a + \beta_c) I_{corr}} \quad (19)$$

The value of R_p increases with increasing JP concentration. A high value of R_p (285.8 Ω cm^2) was noted for 1000 ppm of JP which indicates that the inhibitor passivates the active site on the MS surface. At higher temperatures, R_p values get decreased due to the diffusion of corrosive ions into the active site on the metal atom which follows MS corrosion. Data given in Table 3 also shows that both βa and βc are affected in the presence of inhibitor suggesting both anodic metal dissolution and cathodic hydrogen evolution processes getting influenced by inhibitor JP.

3.5. Computational study

To correlate the inhibition efficiency of JP with its molecular structure, DFT calculations were done. The optimized geometry, FMO (HOMO and LUMO), and electrostatic potential (ESP) map of the JP are presented in Fig. 6. Table 4 contains some of the calculated quantum chemical indices of JP in both the gas and water phase. It is postulated that the inhibitor molecule donates their bonding and non-bonding electrons to the d orbital of Fe atom and simultaneously the back donation of electrons from the filled orbital of metal to the antibonding molecular orbital of the inhibitor molecule causes a synergistic electron transfer between the metal and the inhibitor molecule. Therefore, an inhibitor with a high value of E_{HOMO} and a low value of E_{LUMO} favours strong adsorption and inhibition efficiency. The energy gap (ΔE) is another reactivity parameter that gives an idea about the adsorption tendency and chemical reactivity of the inhibitor molecule [44,45]. In this study, E_{HOMO}, E_{LUMO}, and ΔE values indicate that the JP molecule can act as a good corrosion inhibitor for MS in 0.5 M HCl by adsorbing firmly on the metal surface. Moreover, the ΔN values obtained for pectin in the water phase and gas phase are 0.1049 and 0.1212 respectively. These promising values of electron density propose that the JP possesses a strong tendency for the donation of the bonding and non-bonding electrons to the d orbital of the metal atom. The tendency of replacing the adsorbed water molecules from the metal surface by JP is further evident from the dipole moment values of pectin (4.4902 D) and water (1.85 D). The electrostatic potential (ESP) map of JP in the gas phase was used as a visual tool to determine the more reactive centres in the JP molecule and to estimate the electron density at different regions. In the ESP map (Fig. 6B) the blue colour indicates the most positive (electrophilic) electrostatic potential region and red colour for the most negative (nucleophilic) electrostatic potential region and the green colour region indicate the zero electrostatic potential region [24,46].

3.5.1. Fukui indices

The Fukui functions provide information about the reactive centres in a molecule towards electrophilic and nucleophilic attack. The atomic site for electrophilic attack carrying a positive dual descriptor and nucleophilic attack is controlled by the negative dual descriptor [47,48]. The values of the condensed Fukui functions for electrophilic and nucleophilic attack in the pectin molecule are given in Table S_3. From NBO analysis, it is shown that O (39) will be the most reactive centre for the electrophilic attack and C (29) will be the most reactive site for the nucleophilic attack.

3.5.2. Computational study of protonated pectin

The presence of oxygen heteroatoms in the pectin molecule suggests a tendency for protonation in 0.5 M HCl. In order to detect the most favourable one, geometry optimization of all possible structures with different active oxygen centres for protonation was carried out using the semi-empirical PM6 method. Proton affinity (PA) of a molecule is a measure of their basicity and PA of JP can be calculated from the following equation

Table 3
Parameters obtained from PDP plot of MS in 0.5 M HCl in the absence and presence of different concentration of JP from 303 to 323 K.

Temperature	Conc.of JP (ppm)	I_{corr} (mA/cm^2)	-E_{corr} (mV)	β_a (mV/dec)	β_c (mV/dec)	R_p (Ω cm^2)	CR (mpy)	IE (%)	Standard deviation
303 K	Blank	1.2973	460.56	120.75	223.01	26.21	24.37		
	250	0.4082	440.42	132.32	215.85	87.26	9.703	68.53	0.4983
	500	0.3590	430.95	157.48	226.16	112.3	8.313	72.32	0.8317
	750	0.1450	467.6	107.51	132.02	177.4	5.029	88.82	1.055
	1000	0.1329	446.8	191.6	161.0	285.8	2.392	89.75	0.9937
313 K	Blank	1.4328	471.15	151.6	207.2	26.53	28.06		
	250	0.5315	431.6	138.9	214.9	68.94	11.91	62.90	1.054
	500	0.4550	438.7	133.1	230.4	80.51	10.39	68.24	1.054
	750	0.3140	442.3	143.9	221.4	120.6	8.224	78.08	0.845
	1000	0.2160	466.2	116.7	177.2	141.4	6.549	84.92	0.889
323 K	Blank	1.8923	475.8	125.60	214.38	18.17	36.70		
	250	0.7571	445.8	193.2	254.2	62.95	15.16	59.99	1.056
	500	0.6330	438.4	172.5	200.1	63.54	11.84	66.54	0.547
	750	0.4812	472.9	158.1	184.6	76.84	10.82	74.57	0.628
	1000	0.4450	484.9	155.0	165.9	78.18	9.229	76.48	0.251

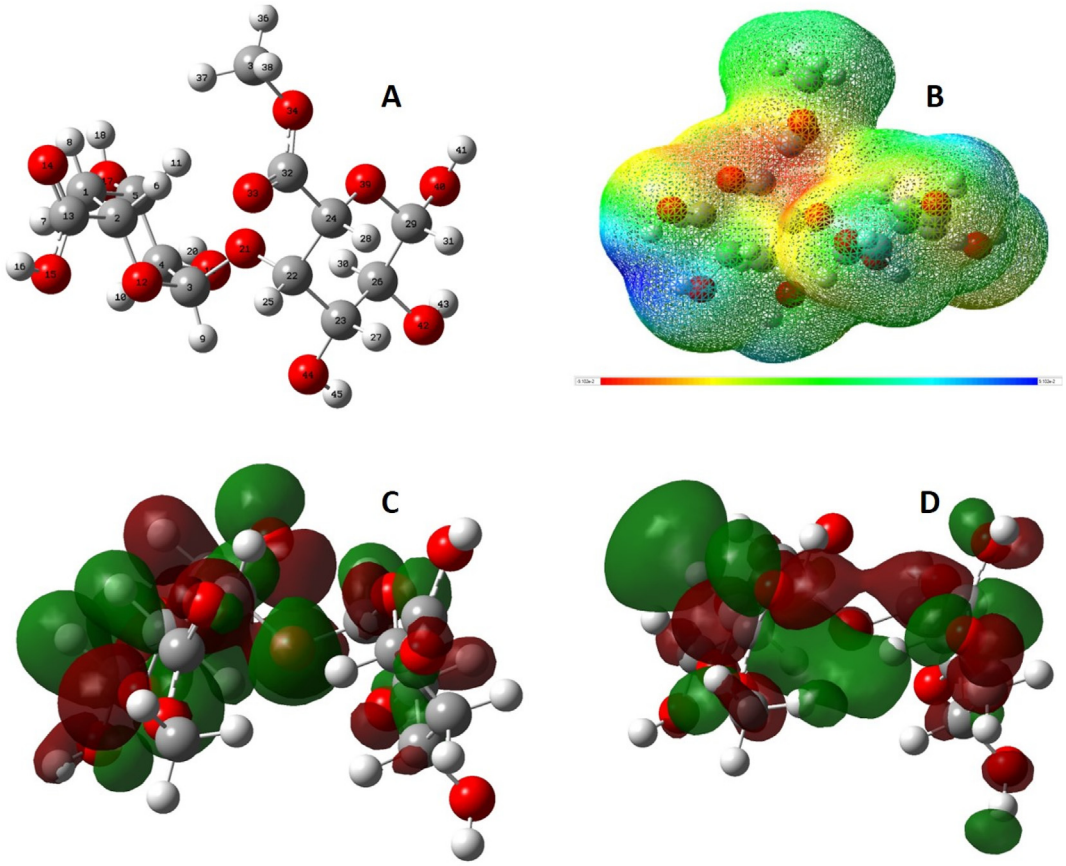

Fig. 6. (A) Optimized geometry, (B) ESP map (C) and (D) FMO of JP.

Table 4
Quantum chemical parameters of JP.

Inhibitor	E_{HOMO} (eV)	E_{LUMO} (eV)	ΔE (eV)	χ (eV)	η (eV)	ΔN
JP (gas phase)	−7.4301	−0.53879	6.8913	3.9844	3.4456	0.1212
JP (water phase)	−7.6013	−0.5611	7.0402	4.0812	3.5201	0.1049
JPH	−9.0179	−5.7190	3.2988	7.3684	1.6494	−0.7725

$$PA = E_{(pro)} - \left(E_{(non-pro)} + E_{H^+}\right) \quad (20)$$

where, $E_{(pro)}$ and $E_{(non\text{-}pro)}$ are the energies of protonated and non-protonated inhibitor molecules. E_H^+ is the energy of H^+ which can be calculated as

$$E_{H^+} = E_{(H_3O^+)} - E_{(H_2O)} \quad (21)$$

In the acidic medium, pectin can accept protons and then interact with the metal surface. A corrosion inhibitor with strong PA can capture proton from the acid media and thus avoid the effect of acid media on metals. So, a strong PA value of a molecule increases its corrosion inhibition efficiency. The proton affinity obtained by protonating at different oxygen atoms is given in Table S_4. It was found that the most probable one with the highest PA value is obtained upon protonation of the oxygen atom (O_{41}) of the pectin molecule. The protonated pectin (JPH) with the highest PA value is then re-optimized using DFT/B3LYP/6-311G (d, p) method. The optimized geometry and FMOs of the JPH are presented in Fig. 7(A-C). The Quantum chemical parameters (Table 4) indicated that E_{HOMO} of JPH is lower compared to E_{HOMO} of JP, which enhances the effectiveness of inhibition. Moreover, the corrosion inhibition performance of JPH is more than unprotonated JP because low ΔE enables adsorption and hence the reactivity of JPH.

3.6. Monte Carlo simulation

To explore the JP adsorption behaviour on MS in the atomic scale, MC simulation has been carried out. The most stable low-energy absorption of studied inhibitor JP on Fe (110)/$4H_3O^+$, $4Cl^-$ ions $190H_2O$ molecule system are given in Fig. 7D. The final visualized snapshots in the acidic medium indicated that the JP molecule could adsorb on the metal surface by aligning parallel to the Fe(110) surface and form a corrosion-protective film of JP. The different parameters gained by the MC simulation study are given in Table S_5. The high negative value of total energy signifies the most stable interaction and easiness of adsorption process. The adsorption energy is defined as the sum of the rigid adsorption energy and the deformation energy for the adsorbate component. (dEad/dNi) reports the energy of metal substrate-adsorbate configurations where one of the adsorbate components has been removed. The adsorption energy values qualitatively state their adsorption capability and further corrosion inhibition performance. The higher adsorption energy of JP inhibitor is a result of the strong interaction of electron rich oxygen atoms with vacant d orbital of Fe atom. Thus, JP could form a barrier film on the Fe (110) surface [49]. The high negative differential adsorption energy of JP (−183.6 kJ/mol) compared to water molecules (−16.56 kJ/mol) indicates the stronger adsorption capacity of pectin by replacing the pre-adsorbed water molecule from the metal surface [46].

3.7. FESEM and AFM

In order to gather visual evidence on the corrosion inhibition performance of the inhibitor JP on MS in 0.5 M HCl, surface characterization was carried out using FESEM and AFM analysis. The morphological

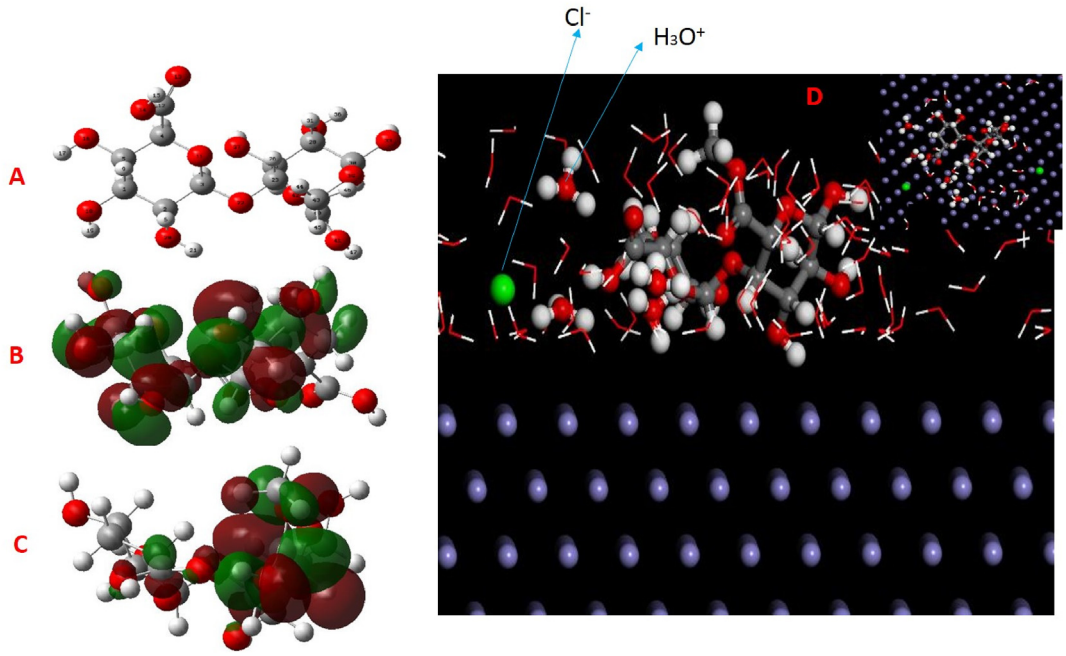

Fig. 7. (A–C) Optimized geometry and FMOs of JPH, (D) Equilibrium adsorption configuration of the JP on the Fe (110) surface in solution obtained by MCs.

changes that occurred on the metal surface on exposure to 24 h in 0.5 M HCl in the absence and presence of 1000 ppm of pectin were monitored via FESEM micrographs (Fig. 8A). As the figure shows, the MS in the absence of an inhibitor is highly damaged with cracks and pits due to the direct attack of corrosive ions. This severe damage is drastically reduced in the presence of inhibitor which is evident from the flower-like morphology of polymeric pectin on the MS surface and this layer substantially reduces the diffusion of electrolyte. AFM micrographs were recorded for estimating the surface roughness of the metal after exposure to the corrosive medium for 24 h in the absence and presence of pectin. The surface roughness of MS after 24 h immersion in 0.5 M HCl without pectin is 237.84 nm and with 1000 ppm of pectin the value changed to 25.36 nm (Fig. 8B). The lowering of surface roughness in the presence of pectin is due to the development of protective film on the MS surface by substituting the pre-adsorbed water molecules.

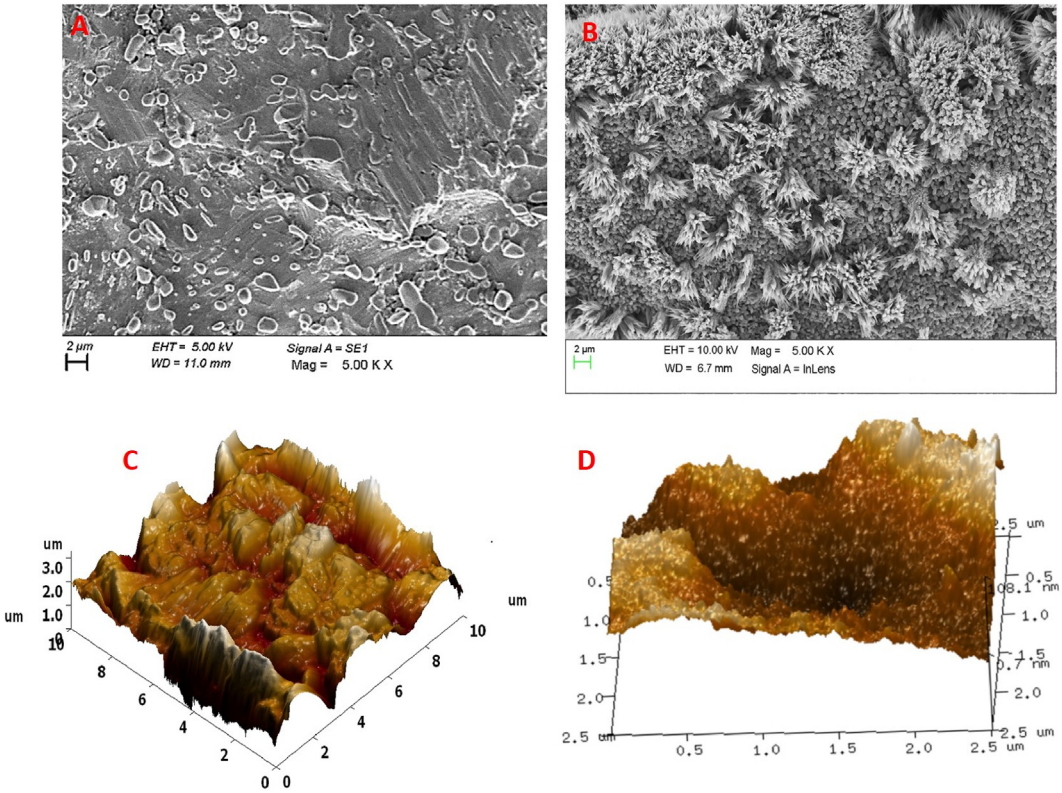

Fig. 8. (A and C) FESEM and AFM images of MS in the absence of JP and (B and D) in the presence of 1000 ppm of JP after 24 h of immersion in 0.5 M HCl.

4. Conclusions

Pectin isolated from the jack fruit peel waste acted as a green corrosion inhibitor for MS in 0.5 M HCl. The IE increased with increasing JP concentration and decreased with increasing temperature. The inhibitor acted as a mixed type by suppressing both anodic metal dissolution and cathodic hydrogen evolution and the adsorption follows the Langmuir isotherm model. The surface modification of the metal in the presence of JP was confirmed by FTIR, SEM, and AFM studies. Quantum chemical studies provided more detailed input on the mode of donor-acceptor interaction and the MC simulation further confirmed that the JP adsorbed on the MS surface by horizontal orientation of active species in JP by replacing the pre-adsorbed water molecules and develops extra corrosion resistance.

Declaration of competing interest

The authors declare that they have no known competing financial interests or personal relationships that could have appeared to influence the work reported in this paper.

Appendix A. Supplementary data

Supplementary data to this article can be found online at https://doi.org/10.1016/j.jics.2021.100271.

References

[1] Thompson NG, Yunovich M, Dunmire D. Cost of corrosion and corrosion maintenance strategies. Corrosion Rev. 2007;25:247–62.
[2] Shainy K, Ammal PR, Unni K, Benjamin S, Joseph A. Surface interaction and corrosion inhibition of mild steel in hydrochloric acid using pyoverdine, an eco-friendly bio-molecule. Journal of Bio-and Tribo-Corrosion 2016;2:1–12.
[3] ElBelghiti M, Karzazi Y, Dafali A, Hammouti B, Bentiss F, Obot I, Bahadur I, Ebenso E-E. Experimental, quantum chemical and Monte Carlo simulation studies of 3, 5-disubstituted-4-amino-1, 2, 4-triazoles as corrosion inhibitors on mild steel in acidic medium. J. Mol. Liq. 2016;218:281–93.
[4] Murulana LC, Kabanda MM, Ebenso EE. Investigation of the adsorption characteristics of some selected sulphonamide derivatives as corrosion inhibitors at mild steel/hydrochloric acid interface: experimental, quantum chemical and QSAR studies. J. Mol. Liq. 2016;215:763–79.
[5] Anupama K, Ramya K, Shainy K, Joseph A. Adsorption and electrochemical studies of Pimenta dioica leaf extracts as corrosion inhibitor for mild steel in hydrochloric acid. Mater. Chem. Phys. 2015;167:28–41.
[6] Thomas A, Prajila M, Shainy K, Joseph A. A green approach to corrosion inhibition of mild steel in hydrochloric acid using fruit rind extract of Garcinia indica (Binda). J. Mol. Liq. 2020:113369.
[7] Dahmani M, Et-Touhami A, Al-Deyab S, Hammouti B, Bouyanzer A. Corrosion inhibition of C38 steel in 1 M HCl: a comparative study of black pepper extract and its isolated piperine. Int. J. Electrochem. Sci 2010;5:1060–9.
[8] Khan M, Abdullah M, Mahmood A, Al-Mayouf AM, Alkhathlan HZ. Evaluation of Matricaria aurea extracts as effective anti-corrosive agent for mild steel in 1.0 M HCl and isolation of their active ingredients. Sustainability 2019;11:7174.
[9] Umoren SA, Eduok UM. Application of carbohydrate polymers as corrosion inhibitors for metal substrates in different media: a review. Carbohydr. Polym. 2016;140:314–41.
[10] Grassino AN, Halambek J, Djaković S, Brnčić SR, Dent M, Grabarić Z. Utilization of tomato peel waste from canning factory as a potential source for pectin production and application as tin corrosion inhibitor. Food Hydrocolloids 2016;52:265–74.
[11] Halambek J, Cindrić I, Grassino AN. Evaluation of pectin isolated from tomato peel waste as natural tin corrosion inhibitor in sodium chloride/acetic acid solution. Carbohydr. Polym. 2020;234:115940.
[12] Subarkah CZ, Chusni MM, Gusniar OW, Sundari CDD. Inquiry-based worksheet on the utilization of pectin from lemon peel waste as corrosion inhibitors to support student understanding in electrochemistry concept. Int. J. Pure Appl. Math. 2018;118:1–15.
[13] Ma X, Wang J, Xu J, Jing J, Li J, Zhu H, Yu S, Hu Z. Sunflower head pectin with different molecular weights as promising green corrosion inhibitors of carbon steel in hydrochloric acid solution. ACS Omega 2019;4:21148–60.
[14] Xu S-Y, Liu J-P, Huang X, Du L-P, Shi F-L, Dong R, Huang X-T, Zheng K, Liu Y, Cheong K-L. Ultrasonic-microwave assisted extraction, characterization and biological activity of pectin from jackfruit peel. Lebensm. Wiss. Technol. 2018;90:577–82.
[15] F. Akter, M. Haque, JACKFRUIT WASTE: A PROMISING SOURCE OF FOOD AND FEED.
[16] Begum R, Aziz M, Uddin M, Yusof Y. Characterization of jackfruit (Artocarpus heterophyllus) waste pectin as influenced by various extraction conditions. Agricult. Agricult. Sci. Procedia 2014;2:244–51.
[17] Koh P, Leong C, Noranizan M. Microwave-assisted extraction of pectin from jackfruit rinds using different power levels. Int. Food Res. J. 2014;21.
[18] Sundarraj AA, Vasudevan RT, Sriramulu G. Optimized extraction and characterization of pectin from jackfruit (Artocarpus integer) wastes using response surface methodology. Int. J. Biol. Macromol. 2018;106:698–703.
[19] Chandel V, Vaidya D, Kaushal M, Gupta A, Verma AK. Standardization of eco-friendly technique for extraction of pectin from apple pomace. Indian J. Nat. Prod. Resour. (IJNPR)[Formerly Natl. Prod. Rad. (NPR)] 2016;7:69–73.
[20] A.C.G.-o.C.o. Metals. Standard Practice for Laboratory Immersion Corrosion Testing of Metals. ASTM International; 2004.
[21] Ranganna S. Handbook of Analysis and Quality Control for Fruit and Vegetable Products. Tata McGraw-Hill Education; 1986.
[22] Shamsheera K, Prasad AR, Jaseela P, Joseph A. Development of Self-Assembled Monolayer of Stearic Acid Grafted Chitosan on Mild Steel and Inhibition of Corrosion in Hydrochloric Acid. Chemical Data Collections; 2020. p. 100402.
[23] Ammal PR, Prajila M, Joseph A. Effect of substitution and temperature on the corrosion inhibition properties of benzimidazole bearing 1, 3, 4-oxadiazoles for mild steel in sulphuric acid: physicochemical and theoretical studies. J. Environ. Chem. Eng. 2018;6:1072–85.
[24] Shamsheera K, Anupama RP, Abraham J. Computational simulation, surface characterization, adsorption studies and electrochemical investigation on the interaction of guar gum with mild steel in HCl environment. Res. Chem. 2020:100054.
[25] Martinez S. Inhibitory mechanism of mimosa tannin using molecular modeling and substitutional adsorption isotherms. Mater. Chem. Phys. 2003;77:97–102.
[26] Kokalj A. On the HSAB based estimate of charge transfer between adsorbates and metal surfaces. Chem. Phys. 2012;393:1–12.
[27] Lgaz H, Chung I-M, Salghi R, Ali IH, Chaouiki A, El Aoufir Y, Khan MI. On the understanding of the adsorption of Fenugreek gum on mild steel in an acidic medium: insights from experimental and computational studies. Appl. Surf. Sci. 2019;463:647–58.
[28] Sánchez-Márquez J, Zorrilla D, Sánchez-Coronilla A, Desireé M, Navas J, Fernández-Lorenzo C, Alcántara R, Martín-Calleja J. Introducing "UCA-FUKUI" software: reactivity-index calculations. J. Mol. Model. 2014;20:2492.
[29] Akhtari K, Hassanzadeh K, Fakhraei B, Fakhraei N, Hassanzadeh H, Zarei SA. A density functional theory study of the reactivity descriptors and antioxidant behavior of Crocin. Comput. Theor. Chem. 2013;1013:123–9.
[30] Villemin D, Abbaz T, Bendjeddou A. Structure, Electronic Properties, NBO, NLO and Chemi-Cal Reactivity of Bis (1, 4-dithiafulvalene) Derivatives: Functional Density Theory Study. 2017.
[31] Singh A, Ansari K, Kumar A, Liu W, Songsong C, Lin Y. Electrochemical, surface and quantum chemical studies of novel imidazole derivatives as corrosion inhibitors for J55 steel in sweet corrosive environment. J. Alloys Compd. 2017;712:121–33.
[32] Sun H. COMPASS: an ab initio force-field optimized for condensed-phase applications overview with details on alkane and benzene compounds. J. Phys. Chem. B 1998;102:7338–64.
[33] John S, Joseph A, Sajini T, Jose AJ. Corrosion inhibition properties of 1, 2, 4-Hetrocyclic Systems: electrochemical, theoretical and Monte Carlo simulation studies. Egypt. J. Petrol. 2017;26:721–32.
[34] Govindaraj D, Rajan M, Hatamleh AA, Munusamy MA. From waste to high-value product: jackfruit peel derived pectin/apatite bionanocomposites for bone healing applications. Int. J. Biol. Macromol. 2018;106:293–301.
[35] Arollado EC, Ponsaran KMG, Loquias MM. Isolation and characterization of pectin from the ripe fruit peels of jackfruit (artocarpus heterophyllus lam.). Acta Med. Philipp. 2018:52.
[36] Dagdag O, Safi Z, Wazzan N, Erramli H, Guo L, Mkadmh AM, Verma C, Ebenso E, El Gana L, El Harfi A. Highly functionalized epoxy macromolecule as an anti-corrosive material for carbon steel: computational (DFT, MDS), surface (SEM-EDS) and electrochemical (OCP, PDP, EIS) studies. J. Mol. Liq. 2020;302:112535.
[37] de Lima KCdS, Paiva VM, Perrone D, Ripper B, Simoes G, Rocco MLM, da Veiga AG, D'Elia E. Glycine max meal extracts as corrosion inhibitor for mild steel in sulphuric acid solution. J. Mater. Res. Technol. 2020;9:12756–72.
[38] Shamsheera K, Prasad AR, Joseph A. Extended protection of mild steel in saline and acidic environment using stearic acid grafted chitosan preloaded with mesoporous-hydrophobic silica (mhSiO2). Surf. Coating. Technol. 2020:126350.
[39] Fekry A, Mohamed RR. Acetyl thiourea chitosan as an eco-friendly inhibitor for mild steel in sulphuric acid medium. Electrochim. Acta 2010;55:1933–9.
[40] Tang Y, Zhang F, Hu S, Cao Z, Wu Z, Jing W. Novel benzimidazole derivatives as corrosion inhibitors of mild steel in the acidic media. Part I: gravimetric, electrochemical, SEM and XPS studies. Corrosion Sci. 2013;74:271–82.
[41] Fiori-Bimbi MV, Alvarez PE, Vaca H, Gervasi CA. Corrosion inhibition of mild steel in HCL solution by pectin. Corrosion Sci. 2015;92:192–9.
[42] Bentiss F, Lebrini M, Lagrenée M. Thermodynamic characterization of metal dissolution and inhibitor adsorption processes in mild steel/2, 5-bis (n-thienyl)-1, 3, 4-thiadiazoles/hydrochloric acid system. Corrosion Sci. 2005;47:2915–31.
[43] Ko S, Prasad AR, Garvasis J, Basheer SM, Joseph A. Stearic acid grafted chitosan/epoxy blend surface coating for prolonged protection of mild steel in saline environment. J. Adhes. Sci. Technol. 2019;33:2250–64.
[44] Arslan T, Kandemirli F, Ebenso EE, Love I, Alemu H. Quantum chemical studies on the corrosion inhibition of some sulphonamides on mild steel in acidic medium. Corrosion Sci. 2009;51:35–47.
[45] Obot I, Obi-Egbedi N. Theoretical study of benzimidazole and its derivatives and their potential activity as corrosion inhibitors. Corrosion Sci. 2010;52:657–60.

[46] Kaya S, Tüzün B, Kaya C, Obot IB. Determination of corrosion inhibition effects of amino acids: quantum chemical and molecular dynamic simulation study. J. Taiwan Inst. Chem. Eng. 2016;58:528–35.
[47] Ramya K, Mohan R, Anupama K, Joseph A. Electrochemical and theoretical studies on the synergistic interaction and corrosion inhibition of alkyl benzimidazoles and thiosemicarbazide pair on mild steel in hydrochloric acid. Mater. Chem. Phys. 2015;149:632–47.
[48] Verma C, Olasunkanmi LO, Ebenso EE, Quraishi MA, Obot IB. Adsorption behavior of glucosamine-based, pyrimidine-fused heterocycles as green corrosion inhibitors for mild steel: experimental and theoretical studies. J. Phys. Chem. C 2016;120: 11598–611.
[49] Lachiri A, El Faydy M, Benhiba F, Zarrok H, El Azzouzi M, Zertoubi M, Azzi M, Lakhrissi B, Zarrouk A. Inhibitor effect of new azomethine derivative containing an 8-hydroxyquinoline moiety on corrosion behavior of mild carbon steel in acidic media. Int. J. Corros. Scale Inhib. 2018;7:609–32.